The efficient monochromatic 800 nm near-infrared emission from Tm^{3+}-doped $NaYbF_4$ upconversion luminescence nanoparticles

XIN YANG[*], LUFANG GUO, YUANHUI ZUO[a], JING LI, HONGCHEN MOU[b,*]
Public Experiment Center, University of Shanghai for Science and Technology, Shanghai 200093, China
[a]*School of Environment and Architecture, University of Shanghai for Science and Technology, Shanghai 200093, China*
[b]*Harbin Normal University, Harbin 150025, China*

The $NaYbF_4$:Tm^{3+}/$NaYF_4$ core/shell upconversion luminescence nanoparticles (UCNPs) with different Tm^{3+}-doped concentrations are synthesized via solvothermal method to obtain efficient monochromatic 800 nm emission under 970 nm excitation. The results indicate that the monochromaticity of 800 nm emission from the UCNPs exhibits exponential growth, while the intensity presents exponential attenuation with increasing Tm^{3+}-doped concentration. The optimal Tm^{3+}-doped concentration in the UCNPs is given, which can be used to generate efficient upconversion emission with high intensity and monochromaticity as high as 1469. The monochromaticity of 800 nm emission calculated by theory is compared with that measured by experiment, and good agreement is found.

(Received May 22, 2015; accepted August 3, 2016)

Keywords: Monochromatic 800 nm emission, $NaYb_{1-x}F_4$:Tm_x^{3+}/$NaYF_4$ nanoparticles, Near-infrared to near-infrared

1. Introduction

Upconversion (UC) is a nonlinear optical process in which sequential absorption of two or more photons of pump light lead to high energy photons [1, 2]. In recent years, upconversion luminescence nanoparticles (UCNPs) have been studied by many researchers because of their unique advantages and promising applications in many fields [3]. For instance, the UCNPs can be used in solidstate laser [4], fluorescent bioprobe [5], bio-imaging [6], and theranostics [7] etc. The advantages of using UCNPs as labels in bio-imaging include eliminating autofluorescence [8], nonblinking [9], multiplex upconversion in vivo bio-imaging [10], and low detection limitations in whole-body animal imaging [11]. The most attractive characteristics of the UCNPs in bio-imaging are the high penetration depth and low absorption in the bio-tissues. If the excitation and emission luminescence are both located in "optical transmission window" (700-1000 nm), it can be well applied to bio-imaging for reducing the autofluorescence [12, 13]. Therefore, the efficient near-infrared to near-infrared (NIR-to-NIR) UC emission is a very promising study.

In terms of rare earth fluoride, Tm^{3+} has a strong peak at 800 nm in NIR region, and Yb^{3+} as a common sensitizer has a great influence on the upconversion efficiency [14, 15]. So several researchers investigated the two ions with different hosts and had achieved some positive results [16-20]. For instance, Chen and his co-workers developed a method to synthesize monodispersed $NaYF_4$:Yb^{3+}, Tm^{3+} nanocrystals with the size ranging from 7 to 10 nm, and came to the conclusion that the increase of Yb^{3+} concentration can enhance the UC emission intensity [17]. Zhang and his co-workers synthesized the $NaYF_4$:Yb^{3+}, Tm^{3+} UCNPs for high-contrast luminescence imaging and concluded that the monochromatic 800 nm emission can be improved by increasing of Tm^{3+}-doped concentration [19]. Wang *et al.* prepared Tm^{3+} and Yb^{3+} co-doped $NaGd(WO_4)_2$ and found that the UC luminescence emission from nanoparticles exhibited pure or virtually pure NIR under excitation of 970 nm [20]. However, to obtain the monochromatic 800 nm emission, the UC emission intensity of the UCNPs is greatly reduced, which results in the limitation of applying the UCNPs to bio-imaging. Therefore, it is significant to explore the relationship between the emission intensity and monochromaticity of 800 nm emission with the change of Tm^{3+}-doped concentration,and improve the intensity on the basis of realizing high monochromaticity.

In present work, $NaYbF_4$ is chosen as host to improve the UC emission intensity and Tm^{3+} is selected as activators to generate monochromatic 800 nm emission under excitation of continuous-wave laser. The $NaYbF_4$:Tm^{3+} UCNPs are coated with a shell of $NaYF_4$ To minimize quenching of the luminescence by surface-associated ligands and surface defects. The uniform $NaYb_{1-x\%}F_4$:$Tm_{x\%}^{3+}$/$NaYF_4$ (x=1, 2, 3, 4) nanoparticles are synthesized and characterized by transmission electron microscopy (TEM). The structural properties and UC emission spectra of the UCNPs are measured by X-ray diffraction (XRD) and UC luminescence spectra respectively. The relationship between the intensity and monochromaticity of 800 nm UC emission from the UCNPs with different Tm^{3+}-doped

concentrations is studied. It is found that when the concentration of Tm^{3+} is 3% for UCNPs, we can obtain efficient UC emission at 800 nm with strong intensity and high monochromaticity. The physical mechanism of $Yb^{3+}$and Tm^{3+} co-doped system is discussed. Furthermore, the monochromaticity of 800 nm emission from the UCNPs is calculated by the steady-state rate equations and compared with experimental result, and the comparison is well consistent.

2. Experimental investigation

2.1 Materials

The experimental materials include $YbCl_3{\cdot}6H_2O$ (99.99%), $YCl_3{\cdot}6H_2O$, $TmCl_3{\cdot}6H_2O$ (99.9%), 1-octadecene (90%), oleic acid (90%), NaOH(>98%), and NH_4F(>98%), which were purchased from Sigma-Aldrich. All of the raw materials were used without any further purification.

2.2 Sample preparation

Based on the solvothermal method [21], $NaYb_{1-x\%}F_4$:$Tm_{x\%}^{3+}$/$NaYF_4$ (x=1, 2, 3, 4) nanoparticles were prepared. Firstly, thulium chloride and ytterbium chloride were weighed and placed in a 50 mL flask containing 15 mL 1-octadecene and 6 mL oleic acid, then the solution was heated to 160 °C and kept for 1 h to dissolve the rare earth by using N_2 as shield gas. Subsequently, the temperature was cooled down to 50 °C, then 3 mL methanol solution containing 0.1 g NaOH and 0.148 g NH_4F was added into the above mixed solution and reacted for 30 min. The methanol and water were removed by evaporation at 100 °C, and then the solution was heated to 305°C and kept for 1.5 h with continuous stirring. Finally, the solution was cooled to the room temperature and the samples were washed by ethanol and cyclohexane for several times. Then, the similar steps were used to realize the core-shell structure. The nanoparticles were obtained by centrifugation and prepared for further use.

2.3 Characterization of sample

The morphology and size of the UCNPs were measured by using FEI Tecnai TF20. The phase of the UCNPs characterized by XRD was measured by Rigaku D/MAX-2600/PC X-ray diffractometer with Cu Kα radiation (λ=1.5406 Å). The UC emission spectra were obtained by monochromator (Zolix Instrument SBP 300) under the excitation of 60 mW power-controlled 970 nm diode laser. The sample was dissolved in cyclohexane, and the power meter was applied to monitor the transmission light to avoid the influence of sample concentration on the spectral measurement. As is the convenience for comparison, all of the compared data were measured at the room temperature.

3. Results and discussion

The TEM of the $NaYb_{1-x\%}F_4$:$Tm_{x\%}^{3+}$/$NaYF_4$ (x=1, 2, 3, 4) UCNPs are shown in Fig. 1. It can be seen that the average diameter of UCNPs synthesized with different Tm^{3+}-doped concentrations is about 25-30 nm and nanoparticles are almost uniform, nearly spherical and monodisperse. Fig. 2 shows the XRD patterns for the UCNPs. The peaks of four samples are well consistent with the standard β-$NaYbF_4$, which indicates that all the samples are pure hexagonal phase and no peaks from other phases or impurities is observed.

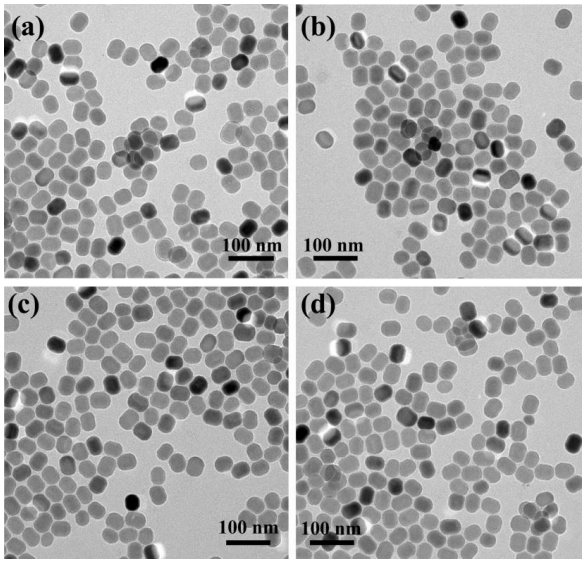

Fig. 1. TEM images of the $NaYb_{1-x\%}F_4$:$Tm_{x\%}^{3+}$/$NaYF_4$ (x=1, 2, 3, 4) UCNPs

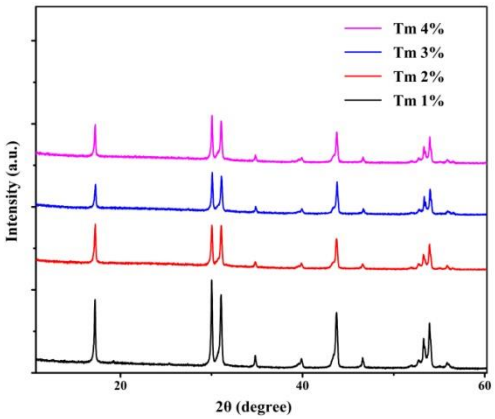

Fig. 2. XRD patterns for the $NaYb_{1-x\%}F_4$:$Tm_{x\%}^{3+}$/$NaYF_4$ (x=1, 2, 3, 4) UCNPs

To investigate the influence of different Tm^{3+}-doped concentrations on the UC emission, the emission spectra of $NaYb_{1-x\%}F_4$:$Tm_{x\%}^{3+}$/$NaYF_4$ (x=1, 2, 3, 4) nanoparticles under excitation of 970 nm diode laser are detected. Fig. 3(a) shows the UC emission spectra of the nanoparticles. It can be seen that there are four UC emission bands centered at 470, 650, 700, and 800 nm, which can be ascribed to

$^1G_4 \rightarrow {}^3H_6$, $^1G_4 \rightarrow {}^3F_4$, $^3F_{2/3} \rightarrow {}^3H_6$, and $^3H_4 \rightarrow {}^3H_6$ transitions of Tm^{3+} ions, respectively [22]. The entire emission intensity gradually decreases with the increase of the Tm^{3+}-doped concentration. In order to make a comparison of the effect of different Tm^{3+}-doped concentrations on the four bands, the 800 nm emission intensity is normalized and shown in Fig. 3(b). It turns out that the 470 nm band ($^1G_4 \rightarrow {}^3H_6$) and the other two bands are greatly influenced by the change of Tm^{3+}-doped concentration.

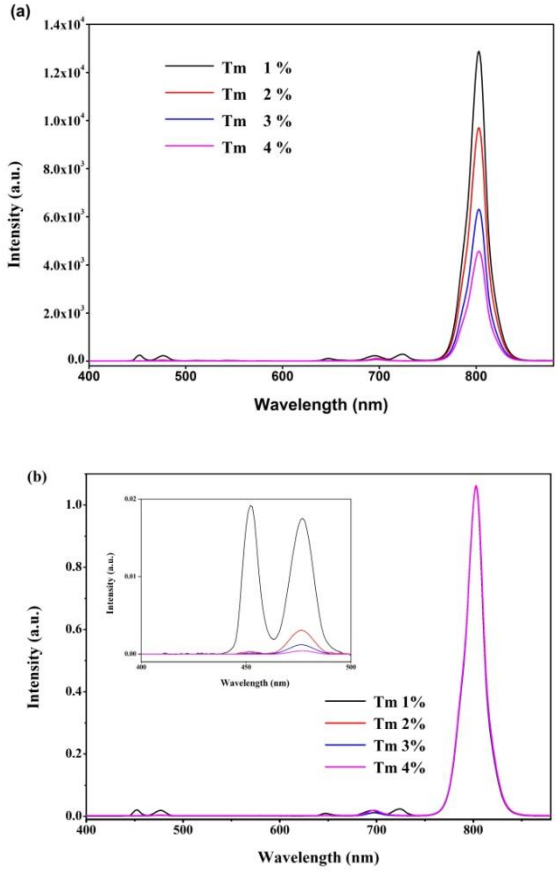

Fig. 3. (a) The UC spectra of the $NaYb_{1-x\%}F_4:Tm_{x\%}^{3+}/NaYF_4$ (x=1, 2, 3, 4) nanoparticles under the excitation of 970 nm laser; (b) The spectra of the nanoparticles in which the peak at 800 nm is normalized

To study the overall UC luminescence emission intensity of the bands, the area of UC bands centered at 470 nm and 800 nm are calculated, respectively. The UC emission intensity of 800 nm (I_{800}) is shown in Fig. 4(a) and it exhibits exponential decay with the increase of the Tm^{3+}-doped concentration. The emission intensity of the UCNPs with 1% Tm^{3+}-doped concentration is very high, which is 3 times stronger than that of 4%. Then, we make a definition of monochromaticity for the 800 nm emission of the UCNPs, which is defined as the ratio of I_{800} and I_{470}, that is, $M=I_{800}/I_{470}$. The monochromaticity is also shown in Fig. 4(a). By contrast with the intensity, the monochromaticity of 800 nm emission presents exponential growth with the increase of Tm^{3+}-doped concentration and the curve can be well fitted by the following equation:

$$M = \frac{I_{800nm}}{I_{470nm}} = 37\exp\left(\frac{C}{0.82}\right) + 45$$

Where C means the concentration of Tm^{3+} ions. When the Tm^{3+}-doped concentration in the UCNPs is 1%, the ratio (M) is 112 and it is 1469 for that of 3%. We can conclude that the increase of emission intensity is at the expense of greatly decreasing the monochromaticity of NIR 800 nm emission. When the Tm^{3+}-doped concentration is 3%, the monochromaticity of 800 nm emission from UCNPs increases by 13 times while the emission intensity reduces by half compared with that of 1%. Therefore, to generate the efficient 800 nm UC emission with strong intensity and high monochromaticity, the optimal concentration of Tm^{3+} in the UCNPs is 3%. The emission spectrum of the UCNPs with 3% Tm^{3+}-doped concentration was shown in Fig. 3(a). It can be seen that the monochromatic 800 nm emission can be generated by the UCNPs and no other peaks can be found in this figure except the peak at 700 nm. As is known, the peak at 700 nm cannot disappear unless the 800 nm emission is very weak. Because the 700 nm emission is still in the region of the "optical transmission window", it has no influence on the application in the bio-imaging.

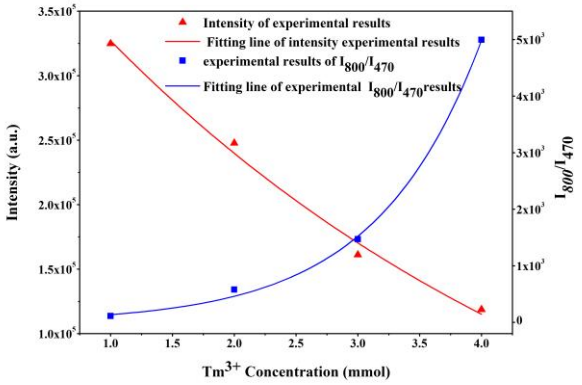

Fig. 4. The relationship between the emission intensity and monochromaticity of 800 nm emission with the change of Tm^{3+}-doped concentration Tm^{3+}-doped concentration

The physical mechanism of Yb^{3+} and Tm^{3+} co-doped system is explained as follows. When $NaYbF_4$ is used as the matrix material, it can substantially enhance the UC emission intensity compared with $NaYF_4$ [23, 24]. As increasing the Tm^{3+}-doped concentration and decreasing Yb^{3+}-doped concentration, the distance between Yb^{3+} ions and Tm^{3+} ions greatly increases while the Tm^{3+} ions decreases. Consequently, the energy transfer process decreases by luminescence quenching of Tm^{3+} ions and the overall UC luminescence intensity becomes weak. Meanwhile, the closeness of the Tm^{3+} ions also enhances the cross-relaxation between $^1G_4 \rightarrow {}^3H_4$ of Tm^{3+} ions and $^3F_4 \rightarrow {}^3F_2$ of Yb^{3+} ions (as shown in Fig. 5). It means that fewer photons are in $^1G_4$ state, while more photons are in $^3H_4$ state. According to the energy level of the Yb^{3+} and

Tm^{3+} co-doped system [25], the monochromatic 800 nm emission are enhanced as the photons population changes.

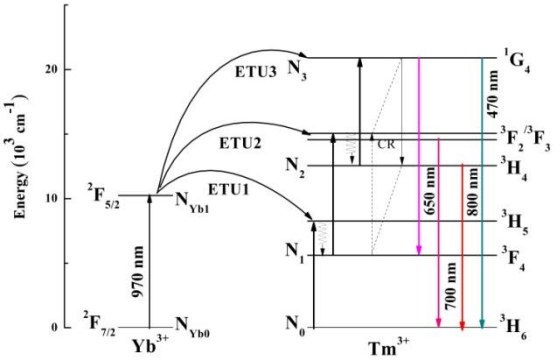

Fig. 5. Energy levels diagram of the Yb^{3+} and Tm^{3+} co-doped system and the process under excitation of 970nm diode laser

Then, the steady-state rate equations are used to calculate the theoretical monochromaticity of 800 nm emission from the UCNPs, which are given as [26]:

$$\frac{dN_{\mathrm{Yb1}}}{dt} = 0 = \rho\sigma_{\mathrm{Yb}}N_{\mathrm{Yb0}} - W_0N_{\mathrm{Yb1}}N_0 - W_1N_{\mathrm{Yb1}}N_1 - W_2N_{\mathrm{Yb1}}N_2 - \frac{N_{\mathrm{Yb1}}}{\tau_{\mathrm{Yb1}}} \quad (1)$$

$$\frac{dN_1}{dt} = 0 = W_0N_{\mathrm{Yb1}}N_0 - W_1N_{\mathrm{Yb1}}N_1 - \frac{N_1}{\tau_1} \quad (2)$$

$$\frac{dN_2}{dt} = 0 = W_1N_{\mathrm{Yb1}}N_1 - W_2N_{\mathrm{Yb1}}N_2 - \frac{N_2}{\tau_2} \quad (3)$$

$$\frac{dN_3}{dt} = 0 = W_2N_{\mathrm{Yb1}}N_2 - \frac{N_3}{\tau_3} \quad (4)$$

where N_i (i=0, 1, 2, 3) and N_{Ybi} (j=0, 1) are the populations of Tm^{3+} ions at the $^3H_6$, $^3F_4$, $^3H_4$, $^1G_4$ states and the populations of Yb^{3+} ions at $^2F_{7/2}$, $^2F_{5/2}$ states, respectively; W_i (i=0, 1, 2) are the rates of the energy transferred from the excited Yb^{3+} ions to the $^3H_6$, $^3F_4$ and $^3H_4$ states of Tm^{3+} ions respectively; σ_{Yb} denotes the absorption cross section of the Yb^{3+} ions; τ_i (i=0, 1, 2, 3) are the lifetimes of relevant energy levels; ρ is the laser photon number density.

Because the decay rates of relevant energy levels are much higher than the upconversion rates [27], we can omit the $W_1N_{\mathrm{Yb1}}N_1$ in Eq. (2) and $W_2N_{\mathrm{Yb1}}N_2$ in Eq. (3). And all upconversion terms in Eq. (1) are negligible compared with the laser pumping. By some algebraic operations, we can obtain the emission intensity:

$$I_{800} \propto N_2 = \rho^2\sigma_{Yb}{}^2W_0W_1N_0\left(N_{Yb0}\tau_{Yb1}\right)^2\tau_1\tau_2 \quad (5)$$

$$I_{470} \propto N_3 = \rho^3\sigma_{Yb}{}^3W_0W_1W_2N_0\left(N_{Yb0}\tau_{Yb1}\right)^3\tau_1\tau_2\tau_3 \quad (6)$$

and the monochromaticity:

$$M = \frac{I_{800}}{I_{470}} \propto \frac{1}{\rho\sigma_{Yb}W_2N_{Yb0}\tau_{Yb1}\tau_3} \quad (7)$$

here ρ , σ_{Yb} , and W_2 can be considered as constants for the sample we prepared. Therefore the monochromaticity ratio of can be written as:

$$\frac{M_x}{M_1} \propto \frac{N_{Yb0_1}\tau_{Yb1_1}\tau_{3_1}}{N_{Yb0}\tau_{Yb1_x}\tau_{3_x}} \quad (8)$$

where M_x *re*presents the monochromaticity of 800 nm emission of the $NaYb_{1\text{-}x\%}F_4{:}Tm_{x\%}{}^{3+}/NaYF_4$ (x=1, 2, 3, 4) UCNPs, which has been defined above.

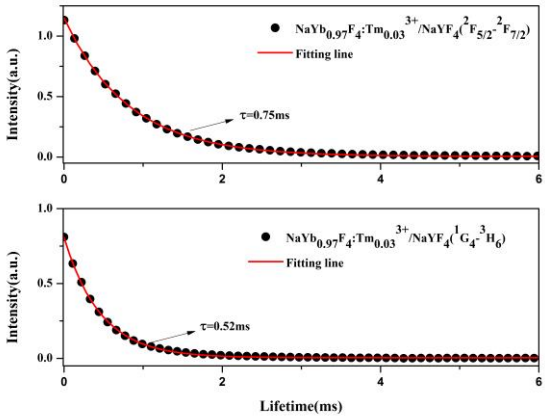

Fig. 6. Time-resolved spectra of $^1G_4 \rightarrow {}^3H_6$ of Tm^{3+} and $^2F_{5/2} \rightarrow {}^2F_{7/2}$ of Yb^{3+} transitions in $NaYb_{0.97}F_4{:}Tm_{0.03}{}^{3+}/NaYF_4$ UCNPs

Table 1. The measurement of lifetimes and the comparison of the monochromaticity ratio of the UCNPs calculated by theory and that measured by experiment

Concentration Tm^{3+} (mol %)	Concentration Yb^{3+} (mol %)	τ_{Yb} (ms)	τ_3 (ms)	Monochromaticity ratio	
				$N_{Yb0}\tau_{\mathrm{Yb1}}\tau_3$	Experimental result
1	99	1.68	0.89	1	1
2	98	1.23	0.78	7	9
3	97	0.75	0.52	18	23
4	96	0.34	0.16	30	79

In order to compare the monochromaticity of 800 nm emission measured by experiment with that calculated by theory, we measure a series of excited-state lifetimes of Yb^{3+} ions and $^1G_4$ state lifetimes of Tm^{3+} ions in the UCNPs with different concentrations. The data of the lifetimes are shown in Table1 which correspond well with the previously reports [19,28]. The radiative time-resolved spectra of the UCNPs with 3% Tm^{3+}-doped concentration are shown in Fig. 6.

It can be seen that the ratios of the monochromaticity of 800 nm emission measured by experiment well agree with that calculated by Eq. (8). But the experimental values are a bit greater than the theoretical results in some cases. It is due to the fact that W_2 is assumed to be a constant in Eq. (7). However, compared with the effect of the decrease of Yb^{3+} concentration, the increase of Tm^{3+}-doped concentration has a great influence on the monochromaticity. It indicates that we cannot assume W_2 as a constant for the UCNPs with different Tm^{3+}-doped concentrations. So Eq. (8) should be modified as:

$$\frac{M_x}{M_1} \propto \frac{W_{2_1} N_{Yb0_1} \tau_{\mathrm{Yb}1_1} \tau_{3_1}}{W_{2_x} N_{Yb0_x} \tau_{\mathrm{Yb}1_x} \tau_{3_x}} \tag{9}$$

As well known, the distance between Yb^{3+} and Tm^{3+} ions become longer with the increase of Tm^{3+}-doped concentration. The longer distance leads to the concentration quenching effect, meanwhile, results in energy transfer process decreasing. Therefore, we can conclude that $W_{2_1} > W_{2_x}$. This can well explain why the theoretical value is bit smaller than the experimental results.

4. Conclusions

In summary, the $NaYbF_4$:Tm^{3+}/$NaYF_4$ core/shell UCNPs with different Tm^{3+}-doped concentrations are synthesized using solvothermal method. The UC emission spectra of the UCNPs are studied. The results show that the intensity of UC emission at 800 nm presents exponential decay while the monochromaticity exhibits exponential growth with the increase of Tm^{3+}-doped concentration. When the Tm^{3+}-doped concentration is 3%, the monochromaticity of 800 nm emission from the UCNPs increases by 13 times while the emission intensity reduces by half compared with that of 1%. The monochromaticity of UC emission at 800 nm is calculated by using steady-state rate equations and compared with experimental results, and good agreement is found. Therefore, the $NaYb_{0.97}F_4$:$Tm_{0.03}{}^{3+}$/$NaYF_4$ UCNPs can be used to generate the efficient 800 nm UC emission with strong intensity and high monochromaticity. It could be well applied to bio-imaging, fluorescent bioprobe, and theranostics.

References

[1] F. Auzel, Chem. Rev. **104**,139 (2004).
[2] F. Wang, X. G. Liu, Chem. Soc. Rev. **38**, 976 (2009).
[3] J. Zhou, Q. Liu, W. Feng, Y. Sun, F. Y. Li, Chem. Rev. **115**, 395 (2015).
[4] G. Rumbles, Nature **409**, 572 (2001).
[5] P. Zhang, S. Rogelj, K. Nguyen, D. Wheeler, J. Am. Chem. Soc. **128**, 12410 (2006).
[6] Y. Liu, M. Chen, T. Y. Cao, Y. Sun, C. Y. Li, Q. Liu, T. S. Yang, L. M. Yao, W. Feng, F. Y. Li, J. Am. Chem. Soc. **135**, 9869 (2013).
[7] G. Y. Chen, H. G. Qiu, Paras N. Prasad, X. Y. Chen, Chem. Rev. **114**, 5161 (2014).
[8] M. X. Yu, F. Y. Li, Z. G. Chen, H. Hu, C. Zhan, H. Yang, C. H. Huang, Anal. Chem. **81**, 930 (2009).
[9] Y. I. Park, J. H. Kim, K. T. Lee, K. S. Jeon, H. Bin Na, J. H. Yu, H. M. Kim, N. Lee, S. H. Choi, S. I. Baik, H. Kim, S. P. Park, B. J. Park, Y. W. Kim, S. H. Lee, S. Y. Yoon, I. C. Song, W. K. Moon, Y. D. Suh, T. Hyeon, Adv. Mater. **21**, 4467 (2009).
[10] L. Cheng, K. Yang, S. Zhang, M. S. Shao, S. T. Lee, Z. Liu, Nano. Res. **3**, 722 (2010).
[11] C. Wang, L. Cheng, H. Xu, Z. Liu, Biomaterials **33**, 4872 (2012).
[12] Z. Li, Y. Zhang, Angew. Chem. **118**, 7896 (2006).
[13] Q. Liu, Y. Sun, T. S. Yang, W. Feng, C. G. Li, F. Y. Li, J. Am. Chem. Soc. **133**, 17122 (2011).
[14] L. L. Jiang, H. B. Zhang, S. G. Xiao, X. L. Yang, J. W. Ding, J. Optoelectron. Adv. M. **6**, 547 (2012).
[15] B. S. Cao, Y. Y. He, L. Zhang, B. Dong, J. Lumin. **135**, 128 (2013).
[16] M. Nyk, R. Kumar, T. Y. Ohulchanskyy, E. J. Bergey, P. N. Prasad, Nano Lett. **8**, 3834 (2008).
[17] G. Y. Chen, T. Y. Ohulchanskyy, ACS Nano. **4**, 3163 (2010).
[18] G. Y. Chen, J. Shen, T. Y. Ohulchanskyy, ACS Nano. **6**, 8280 (2012).
[19] J. Y. Zhang, H. Zhao, X. T. Zhang, X. Z. Wang, H. Gao, Z. G. Zhang, W. W. Cao, Phys. Chem. C **118**, 2820 (2014).
[20] Z. F. Wang, Y. Z. Li, Q. Jiang, H. D. Zeng, Z. P. Ci, L.Y. Sun, J. Mater. Chem. C **2**, 4495 (2014).
[21] Y. Cui, S. Zhao, M. Han, P. Li, L. Zhang, Z. Xu, J. Nanosci. Nanotechnol. **14**, 3597 (2014).
[22] J. C. Boyer, L. A. Cuccia, J. A. Capobianco, Nano Lett. **7**, 847 (2007).
[23] X. M. Li, H. Guo, J. Lumin. **152**, 168 (2014).
[24] J. Wang, R. Deng, M. A. MacDonald, B. Chen, J. Yuan, F. Wang, D. Chi, T.S. Hor, P. Zhang, G. Liu, Y. Han, X. G. Liu, Nat. Mater. **13**, 157 (2014).
[25] J. B. Gruber, M. E. Hills, R. M. Macfarlane, C. A. Morrison, G. A. Turner, G. J. Quarles, G. J. Kintz, L. Esterowitz, Phys. Rev. B **40**, 9464 (1989).
[26] H. J. Liang, Y. D. Zheng, L. Wu, L. X. Liu, Z. G. Zhang, W. W. Cao, J. Lumin. **131**, 1802 (2011).
[27] M. Pollnau, D. R. Gamelin, S. R. Lüthi, H. U. Güdel, M. P. Hehlen, Phys. Rev. B **61**, 3337 (2000).
[28] H. L. Qiu, C. H. Yang, W. S, J. Damasco, X. L. Wang, H. A. P. N. Prasad, G. Y. Chen, Nanomaterials. **4**, 55 (2014).

*Corresponding author: shangliyx@usst.edu.cn
hsdmhc@126.com